Shen et al. *NPG Asia Materials* (2021) 13:39
https://doi.org/10.1038/s41427-021-00303-1

NPG Asia Materials

REVIEW ARTICLE Open Access

Strategies to improve photodynamic therapy efficacy by relieving the tumor hypoxia environment

Zijun Shen[1], Qingming Ma[1], Xinyu Zhou[1], Guimin Zhang[2], Guizhou Hao[2], Yong Sun[1] and Jie Cao[1]

Abstract

Photodynamic therapy (PDT) is an emerging technology for tumor treatment in which photosensitizer (PS)-mediated light irradiation reduces oxygen, producing high levels of reactive oxygen species (ROS) that can cause vascular injury and effectively kill tumor cells. However, the naturally hypoxic tumor microenvironment is the main obstacle that hinders the photodynamic response in vivo and prevents its extensive application to tumor treatment. Moreover, PDT-mediated oxygen consumption further increases tumor hypoxia, potentially causing a variety of adverse consequences, such as angiogenesis, tumor invasion, and metastasis. To overcome these limitations caused by hypoxia, multiple strategies have been investigated, including the use of oxygen carriers and reactive oxygen supply materials, the regulation of tumor microenvironments, and multimodal therapy including PDT. In this review, we summarize the latest progress in the development of strategies to relieve tumor hypoxia for improved PDT efficacy and better therapeutic effects.

Introduction

Photodynamic therapy (PDT) has become a major strategy for solid cancer treatment due to its inherent advantages, such as high selectivity, noninvasiveness, and low systemic toxicity. Effective PDT typically involves the use of photosensitizers (PSs), appropriate laser irradiation, and a sufficient oxygen supply[1]. Specifically, the electrons of PS are elevated from the ground state (S0) to the excited state (S1) upon light irradiation and then pass through the excited triplet state (T1) through intersystem crossing, forming free radicals through a type I reaction or transferring energy to the surrounding molecular oxygen ($^3O_2$) to produce highly active singlet oxygen ($^1O_2$), as illustrated schematically in Fig. 1 (ref. [2]). The generated $^1O_2$ and adjacent biological macromolecules undergo oxidative reactions that can further lead to cytotoxicity, cell damage, and even death. While it has numerous advantages, the application of PDT for cancer treatment is limited due to several intrinsic drawbacks. For instance, when subjected to light irradiation, PS will convert oxygen to reactive oxygen species (ROS) with high cytotoxicity, which further aggravates the hypoxia of tumors. Therefore, in addition to pre-existing tumor hypoxia, the effectiveness of PDT will be further deteriorated by the oxygen consumption involved in the generation of ROS[3]. Moreover, the deterioration of tumor hypoxia will further promote cancer progression and metastasis, increasing the risk of PDT resistance[4]. Therefore, proposing new and effective strategies to reduce tumor hypoxia has become a primary research focus for improving PDT efficacy.

Recently, many studies on improving the hypoxic status of tumors to enhance PDT efficacy have been carried out, and significant progress has been made[5–8]. For instance, novel nonreactive oxygen carriers, such as liposome-encapsulated hemoglobin (HB) and perfluorocarbon carbide, have been designed and used[9]. Moreover, reactive

Correspondence: Jie Cao (caojie0829@hotmail.com)
[1]Department of Pharmaceutics, School of Pharmacy, Qingdao University, Qingdao 266021, China
[2]Department of Scientific Research, Lunan Pharmaceutical Corporation, Linyi 276001, China
These authors contributed equally: Zijun Shen, Qingming Ma

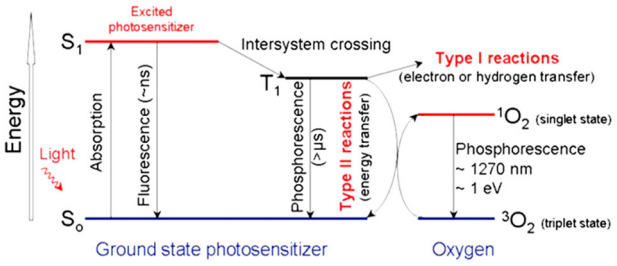

Fig. 1 A Jablonski diagram illustrating the mechanism of photosensitization processes. Copyright 2015, American Cancer Society (ref. [2]).

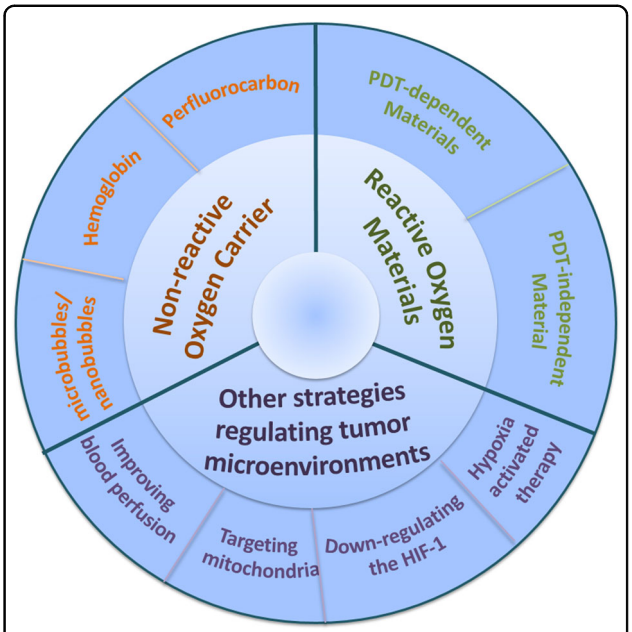

Fig. 2 Summary of the main strategies to improve PDT efficacy by relieving the tumor hypoxic envioronment. Overview of the strategies including the non-reactive oxygen carriers, reactive oxygen supply materials and other strategies regulating tumor microenvironments.

oxygen supply materials, such as metal oxides, hydrogen peroxide (H_2O_2) enzymes, active nanoparticles that can react with acid and H_2O_2 in vivo to produce oxygen, and materials that can produce oxygen under PDT conditions, such as PT(IV) nanocomposites, have also been studied. In addition, other strategies that can alleviate or take advantage of hypoxic environments have also been reported, such as administering hypoxia-inducible factor inhibitors, targeting organelles, increasing blood perfusion, and performing combined therapy with hypoxia-response drugs.

Therefore, a comprehensive and in-depth depiction of the whole scene of the recent development of tumor hypoxia-improving strategies to enhance PDT efficacy, from fundamentals to applications, is desirable. In this review, we summarize the main research strategies in recent years, from the design of novel nonreactive oxygen carriers to reactive materials and other strategies, including the regulation of tumor microenvironments and PDT-involved multimodal therapy, to improve the hypoxic microenvironment to enhance PDT efficacy (Fig. 2).

Nonreactive oxygen carriers

Hemoglobin

HB is one of the major components in red blood cells with inherent reversible oxygen-binding capability and can transport oxygen molecules to tissues. However, as an oxygen donor, cell-free HB presents several problems, including poor stability, short circulation time, and potential side effects[10]. Therefore, the incorporation of HB into hybrid oxygen carriers, such as glutaraldehyde-polymerized HB and poly(ethylene glycol)-conjugated HB (PEG-HB), to form HB-based oxygen carriers (HBOCs) to facilitate PDT has been widely investigated[11–14]. However, most HBOCs cause vascular contraction due to their nitric oxide (NO) scavenging capacity, leading to an unfavorable sharp increase in blood pressure[15]. Compared with HBOCs, oxygen carriers with sizes in the nanometer range can perfuse tumor tissues more efficiently and provide a higher oxygen supply in hypoxic tumors. Many studies on the development of HB-based nano-oxygen carriers have been carried out, and significant progress has been achieved[16,17].

Liposomes have attractive prospects in clinical applications due to their inherent advantages, such as good biocompatibility, targeting ability and drug protection. Recently, liposome-encapsulated HB has been proposed and studied as an oxygen carrier and was found to reduce side effects and enhance the half-life of the HB cycle. For example, as illustrated in Fig. 3, Yang et al.[18] developed a multifunctional liposome with enhanced chemotherapeutic effects by simultaneously incorporating HB as the oxygen carrier and doxorubicin (DOX) as the antitumor drug. First, HB can be cross-bonded in the phospholipid membrane by hydrophobic forces. Then, DOX and HB are loaded into the aqueous phase of the liposome, while part of the HB is connected to the surface of the liposome membrane through hydrophobic interactions to form DOX–HB–liposomes (DHL). The prepared DHL can offer sufficiently high oxygen loading and can perform site-specific delivery of oxygen to tumors, which can improve tumor hypoxia. MTT results indicated that even at a concentration of 150 μg/mL, the cytotoxicity to the test cells was very low; hematoxylin and eosin (H&E) staining results showed that there was no obvious histological damage to normal organs, which further proved the safety and biocompatibility of liposomes.

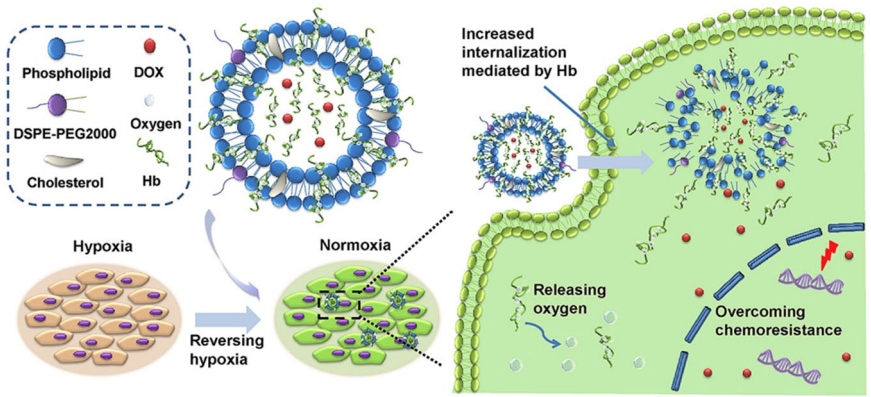

Fig. 3 Schematics illustrating the improvement of tumor hypoxia and enhanced PDT based on synchronous oxygen and DOX delivery by liposomes. Copyright 2018, Elsevier (ref. [18]).

Studies have shown that excessive iron can promote the occurrence and growth of tumors, and many types of cancer cells (such as breast cancer, liver cancer, and colon cancer) upregulate proteins related to iron uptake. Therefore, cancer cells may absorb iron-containing HB more easily, allowing such HB-liposomes to be specifically internalized into cancer cells. Consistently, the results of an in vivo distribution experiment with HBL revealed that compared with liposomes without HB, HBL showed stronger fluorescence at the tumor site, indicating that the HB-mediated drug combination could improve specific uptake into tumor cells. Moreover, under the effect of O_2 interference, hypoxic cancer cells showed an increased capacity to take up the delivered drugs, resulting in significant cancer cell apoptosis. In addition, DHL can markedly increase ROS production in hypoxic tumors and thereby increase the cytotoxicity of DOX, which is typically mediated by ROS. Due to the resultant higher drug and oxygen concentrations in tumor regions, DHL shows great promise in reversing hypoxia-induced chemoresistance and exhibits improved antitumor effects.

In addition, Cai et al.[19] developed biomimetic lipid-polymer nanoparticles (I-ARCs) that can load a special compound assembled from indocyanine green (ICG) as a PS and HB as an oxygen carrier (Fig. 4). The prepared I-ARCs can act as nanosized artificial red blood cells with the ability to generate oxygen and provide real-time monitoring of the PDT process simultaneously. Specifically, I-ARCs consist of biocompatible lipid shells, which were designed to mimic the cell membrane, and poly(D, L-lactic acid-co-glycolic acid) (PLGA) nuclei, in which HB was assembled with ICG to form HB/ICG complexes. Upon 808 nm light irradiation, I-ARCs can produce 9.5 times more ROS than deoxidized ICG nanoparticles. Moreover, since ICG shows fluorescence signals and a photoacoustic response, the biodistribution and metabolism of HB/ICG complex-loaded I-ARCs can be easily monitored during PDT.

Perfluorocarbon

Considering that HB may be susceptible to conformational changes during the chemical modifications involved in the fabrication process of HB-based nanomaterials, other candidates, such as solutions or materials with considerable oxygen storage capacity, would be suitable alternatives. For example, compared with HB, perfluorocarbons (PFCs) can exhibit a higher oxygen solubility (40–56 ml O_2 per 100 ml PFC at 760 Torr and 25 °C)[20,21] and can donate molecular oxygen in the tumor tissue, thereby improving PDT efficiency in the hypoxic region. Recently, many efforts have been made to improve PDT efficacy by adding PFCs in preclinical or clinical research, as summarized in Table 1[22–30]. For instance, Cheng et al.[31] explored oxygen self-enrichment PDT (Oxy-PDT) by loading the PS IR780 into PFC nanodroplets to enhance the PDT effect (Fig. 5). In this system, a continuous oxygen supply facilitates the prolongation of PDT and fully utilizes the efficacy of IR780. The results demonstrated that compared with traditional PDT methods, the tumor growth of mice can be significantly inhibited by intravenously injecting a single dose of Oxy-PDT.

Although PFCs have a high oxygen capacity, the oxygen release efficiency is purely based on oxygen concentration gradient-dependent passive diffusion and is lower than that of HB. To overcome this obstacle, Song et al.[32] developed an ultrasound-triggered tumor oxygenation strategy by using nano-PFC as the oxygen carrier, as shown by the schematics in Fig. 6. A human serum albumin-stabilized PFC nanodroplet system was proposed to regulate tumor-specific oxygen delivery and readily trigger oxygen release by external synchronous ultrasound

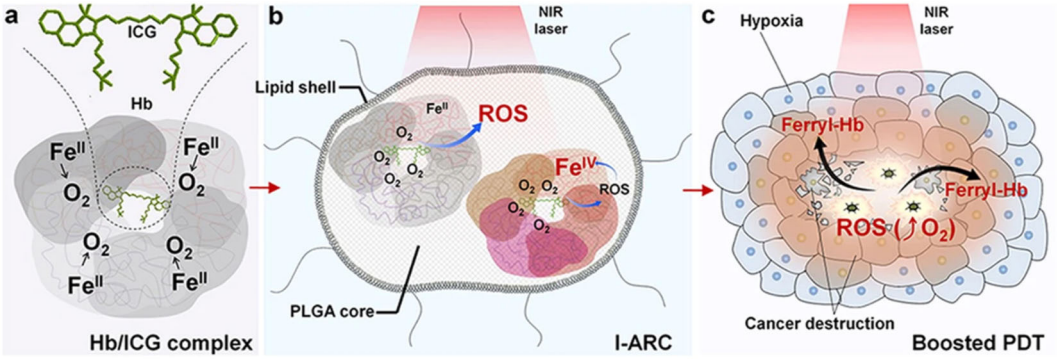

Fig. 4 Schematic illustration of the boosted PDT effect of HB/ICG complex-loaded I-ARCs on cancer. a The formation of HB/ICG complex. **b** The construction of bioinspired I-ARCs. **c** I-ARCs promoted ROS generation under NIR laser. Copyright 2016, Nature Publishing Group (ref. [19]).

Table 1 Studies on using perfluorocarbons to improve PDT efficacy.

Perfluorocarbon	Chemical formula	Status	Delivery system	Combined photosensitizer/drug	Reference
Perfluorohexane	C6F14	Preclinical	Nanodroplet	IR780	22
		Preclinical	Nanoemulsions	fluorous porphyrin	23
		Preclinical	Nanodroplet	Ce6	24
Perfluorotributylamine	C12F27N	Preclinical	Nanoparticles	IR780	25
Perfluorooctyl bromide	C8BrF17	Preclinical	Nanocapsules	IR780	26
		Preclinical	Nanoliposome	ICG	27
		Preclinical	Nanodroplet	Ce6	28
Perfluoropropane	C3F8	Clinical	Gas	Verteporfin	29
Perfluoropentane	C5F12	Preclinical	Nanocubes	HPB	30

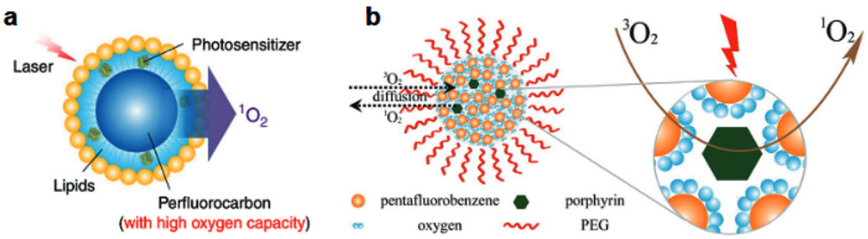

Fig. 5 Schematic illustration of the mechanisms for O_2 delivery via a PFC-lipid core/shell nanostructure and enhancement of PDT efficacy by fluorinated domains. a Structure and design of the Oxy-PDT agent. **b** The meachanism of enhancing the singlet oxygen production via Oxy-PDT. Copyright 2015, Nature Publishing Group (ref. [31]).

therapy. The nanodroplets were intravenously injected into tumor-bearing 4T1 mice, and then the mice were treated with pure oxygen breathing for 30 min and ultrasonication for 30 min. In this process, nanodroplets adsorbed oxygen in the lungs, carried it into tumors through blood circulation, and then released oxygen effectively in the tumors. The level of O_2 in the tumors increased rapidly from 17 to 49%, improving the anti-tumor effect of the PDT regimen.

Oxygen-containing microbubbles/nanobubbles

In addition to HB and PFCs as oxygen carriers, oxygen-loaded microbubbles/nanobubbles have recently been used as a novel potential reagent to provide supplemental

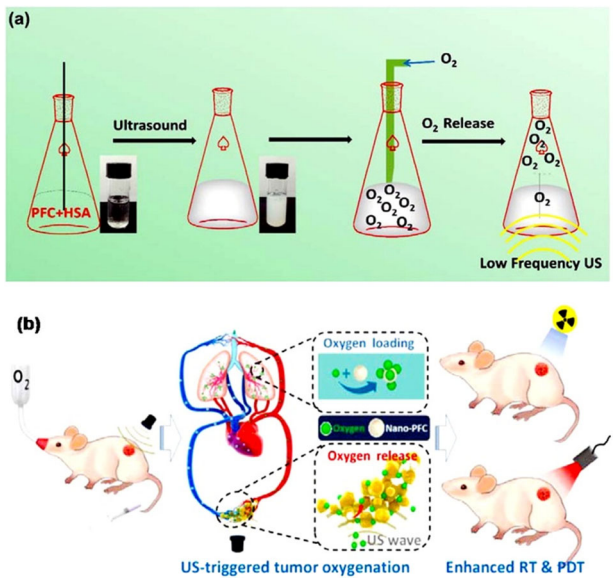

Fig. 6 Preparation of PFC nanoemulsion and illustration of mechanisms for enhancing PDT efficacy with nano-PFCs. a The fabrication of the PFC nanoemulsion. **b** Illustration of the mechanism of oxygen generation triggered under ultrasound (US) waves. Copyright 2016, American Chemical Society (ref. [32]).

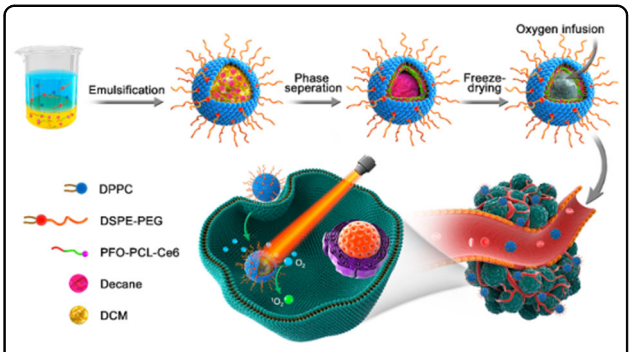

Fig. 7 Illustration of the synthesis and applications of lipid-polymer bilaminar oxygen nanobubbles conjugated with Ce6 in vivo. Copyright 2018, American Chemical Society (ref. [34]).

oxygen in the hypoxic microenvironment of solid tumors[33,34]. These bubbles have excellent biocompatibility and effective and high oxygen-carrying capacity (>70% v/v). The combination of microbubbles/nanobubbles and PSs has been demonstrated to have great potential to enhance therapeutic efficacy in hypoxic tumor models. In general, nanobubbles bound to PS can accumulate in the cytoplasm, and then the PS inside is released by destroying the shell of the bubbles. When the oxygen diffuses out from the shell, the bubble shrinks to a point where the external Laplace pressure breaks the bubble, thereby releasing the PS. Then, the PS generates singlet oxygen under laser irradiation and exerts an efficient PDT effect in a high oxygen environment.

For example, Song et al.[34] designed bilaminar oxygen nanobubbles with chlorin e6 (Ce6) connected to a polymer shell as a new oxygen supply material. The developed oxygen-loaded nanobubbles can provide a large amount of oxygen to improve the therapeutic effect of oxygen-consuming PDT (Fig. 7). The lipid-polymer bilaminar oxygen nanobubbles were prepared using a combination of emulsion solvent evaporation and internal phase separation. Compared with the phospholipids or surfactants used in other oxygen delivery systems, the lipid molecules around the polymer shell selected by the researchers show good biocompatibility. The combination of the hydrophilic polymer PEG and lipid provides an invisible layer of nanocapsules, thereby inhibiting the phagocytosis of mononuclear macrophages and improving the stability of nanocapsules and system circulation life. More importantly, the hydrophobic fluorinated cap at the end of the polycaprolactone polymer provides a strong gas diffusion barrier to reduce the premature release of oxygen before reaching the tumor site. In addition, the polymer shell can withstand higher Laplace pressures, keeping the bubbles at the nanometer scale, thereby enabling the use of enhanced permeability and retention to target tumor cells while maintaining good stability. Moreover, the synthesized nanobubbles have good stability that can inhibit premature oxygen release and can be stored in the form of freeze-dried powders to enable simple pre-use reconstruction, thus solving the storage problems troubled by PFC oxygen delivery systems. Both in vitro and in vivo results showed that PDT treatment with oxygen-containing nanobubbles can greatly enhance the production of singlet oxygen and achieve excellent therapeutic effects.

Reactive oxygen supplementation materials

PDT-dependent materials

In recent years, researchers have prepared PDT-dependent materials for oxygen generation[35,36], which can effectively supplement oxygen in PDT by decomposing nanoparticles under laser irradiation. Pt(IV) is a Pt-based light-activated precursor drug that can be decomposed into oxygen and Pt(II) with anticancer activity under long-wavelength light irradiation. The PS can therefore be assembled with Pt(IV) to form a nanocomplex for photodynamic-chemotherapy combined treatment. For example, Xu et al.[37] designed self-generated multifunctional nanocomposites containing oxygen and Pt(II) to reverse the PDT resistance induced by hypoxia, as illustrated in Fig. 8. The nanocomposites consist of Pt(IV) and Ce6, by which upconversion nanoparticles (UCNP) are loaded to convert near-infrared (NIR) light at 980 nm to light emission at 365 and 660 nm, respectively, further inducing the decomposition of Pt(IV)

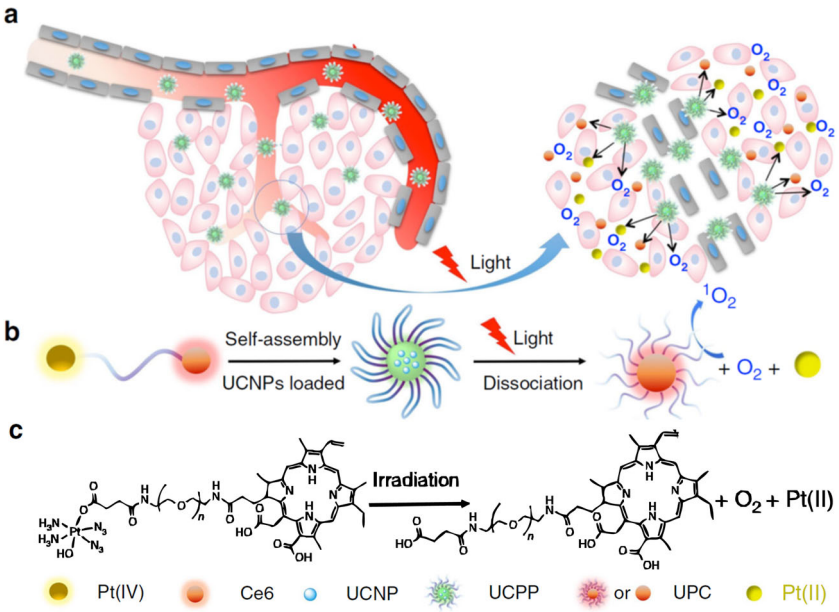

Fig. 8 An overview illustrating the formation and functional mechanism of UCPP nanoparticles. a Light-driven dissociation of UCPP in the tumor microenvironment; **b** formation of UCPP; and **c** light-driven dissociation of UCPP, including O_2 self-generation, the simultaneous activation of PDT, and the release of active Pt(II) for synergistic photochemotherapy. Copyright 2018, Nature Publishing Group (ref. [37]).

and the production of oxygen and thereby properly driving PDT with UCNP-embedded nanoparticles (denoted UCPP). When laser irradiation at 980 nm is used to trigger the decomposition of UCPP, oxygen can be generated through chemical reactions to compensate for oxygen consumption in the PDT process, and active Pt(II) can be released for synergistic photochemistry.

PDT-independent materials

In addition to PDT-dependent materials, PDT-independent materials could generate oxygen through chemical reactions not involved in the PDT process. Various reactive oxygen-generating materials, including metal oxides, catalase-active materials, and water-splitting materials, have been used to overcome hypoxia.

Metal oxide materials

In recent years, metal oxides have been demonstrated to produce oxygen through chemical reactions with acids or H_2O_2 and can effectively alleviate the oxygen consumption in the PDT process[38–41]. Therefore, metal oxides show promise for use along with PSs to improve the efficiency of PDT.

MnO_2 nanomaterials. Manganese oxide (MnO_2) has attracted increasing attention due to its ability to generate excessive oxygen with the aid of acid and H_2O_2 in the tumor microenvironment.

The following reactions illustrate how acid-induced H_2O_2 promotes the degradation of MnO_2 and the resultant generation of oxygen:

$$MnO_2 + 2H^+ \rightarrow Mn^{2+} + H_2O + 1/2O_2; \quad (1)$$

$$MnO_2 + H_2O_2 + 2H^+ \rightarrow Mn^{2+} + 2H_2O + O_2; \quad (2)$$

MnO_2 shows high reactivity and specificity to acidic environments and the presence of H_2O_2, where it can produce oxygen continuously to overcome hypoxia in tumors[42–45]. After reacting with excessive H_2O_2 in an acidic tumor microenvironment, MnO_2 nanosheets can be degraded to produce a large amount of oxygen, thus greatly improving the efficiency of PDT. In addition to increasing the oxygen content, MnO_2 can also be used as a glutathione (GSH) inhibitor in vivo to increase PDT efficacy. Moreover, it can be used to make upconversion nanocomposites to stimulate PSs at various wavelengths to enhance the selectivity of PDT. In addition, Mn^{2+} produced by MnO_2 is a strong T1 magnetic resonance (MR) contrast agent for tumor detection, which can also be used for in site tumor imaging[46,47]. At the same time, it is worth mentioning that, as an essential trace element in the human body, Mn can be adjusted by metabolism, so it has good biocompatibility.

MnO_2 as a GSH inhibitor to replenish oxygen and increase PDT efficacy In addition to low oxygen, the effectiveness of PDT is also limited by the hypoxia-induced

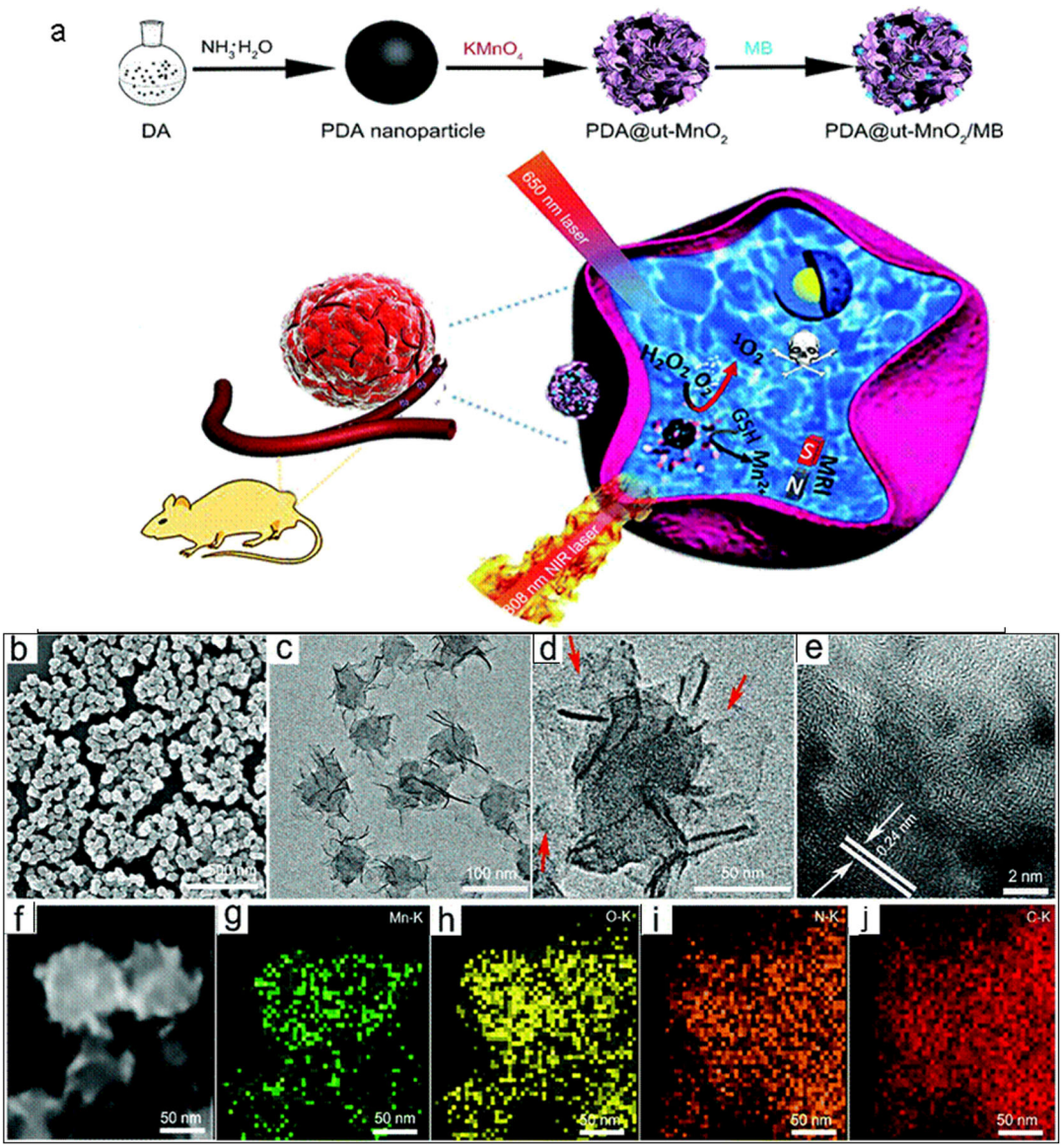

Fig. 9 A simple and convenient method for achieving the controllable growth of ultrathin manganese dioxide nanosheets. a Schematics of the formation and functional mechanism of PDA@ut-MnO_2/MB NFs; **b** SEM micrograph of PDA@ut-MnO_2NFs; TEM micrographs of PDA@ut-MnO_2NFs at **c** low and **d** high resolution (the arrows point out the ultrathin MnO_2 nanosheets); **e** HRTEM micrograph of MnO_2 nanosheets; and **f**–**j** a HAADF-STEM micrograph and elemental mapping of Mn, O, N, and C of PDA@ut-MnO_2 NFs. Copyright 2019, Royal Society of Chemistry (ref. [50]).

overexpression of GSH, which consumes ROS before they reach their target and hence greatly reduces the efficiency of PDT. Numerous studies have attempted to develop a more stable and effective PDT system by the incorporation of GSH depletors[48]. MnO_2 can be used as an efficient glutathione dehydrogenase inhibitor to reduce GSH levels; therefore, a MnO_2-containing PDT system is expected to overcome the drawbacks caused by hypoxia and GSH overexpression at the tumor site[49].

Sun et al.[50] proposed a simple and convenient method for achieving the controllable growth of ultrathin manganese dioxide nanosheets by introducing a redox reaction on polydopamine nanospheres (Fig. 9). The prepared multi-functional polydopamine@ultrathin manganese dioxide/methylene blue (MB) nanoflowers (termed PDA@ut-MnO_2/MB NFs) are suitable platforms for synergistic tumor therapy and can efficiently modulate the tumor microenvironment by generating O_2 and depleting GSH. In addition, they can support ultrasensitive reduction-responsive MR imaging (MRI). The morphology and composition of PDA@ut-MnO_2 were identified and characterized by scanning electron microscopy (SEM),

transmission electron microscopy (TEM), high-resolution transmission electron microscopy (HRTEM) and high-angle annular dark field scanning transmission electron microscopy (HAADF-STEM), and their therapeutic effects were evaluated in mice bearing HCT116 colorectal tumors as models. Tumors were collected 15 days after injection, and PDA@MnO_2/MB showed nearly complete tumor growth inhibition under MRI-guided PDT/PTT cotreatment. The H&E staining results of tumor sections also confirmed serious pathological damage, such as severe nuclear pyknosis and nuclear necrosis. Moreover, MRI of tumor-bearing mice found that the T1-weighted MR signal of the kidney was significantly enhanced 2 h after the injection, and the total manganese content in urine was measured by inductively coupled plasma mass spectrometry (ICP-MS). Approximately 65% of the manganese content was detected, suggesting that Mn^{2+} was eliminated from the body through the kidneys, and the in vivo toxicity was minimal. These results demonstrated that PDA@MnO_2/MB NFs can achieve a high degree of tumor growth suppression under MRI-assisted treatment.

Furthermore, Fan's group[51] developed an intelligent PS-MnO_2 nanosystem, which exhibited high intracellular drug delivery capacity and enhanced PDT efficacy by reducing GSH levels and increasing oxygen content in cancer cells. Specifically, MnO_2 nanosheets act as oxygen supplements and oxidants to reduce intracellular GSH levels. In addition, they have been shown to effectively induce the fluorescence quenching of Ce6 to offer an on–off fluorescence signal for real-time monitoring. In the Ce6-MnO_2 nanosystem, Ce6 can be well protected from light-induced self-destruction and can be effectively transported to the cytoplasm. After endocytosis, MnO_2 nanosheets were reduced by intracellular GSH. The results show that the nanosystem can be disintegrated, generate oxygen, and reduce the GSH level, subsequently inducing 95% cell death when combined with Ce6. Moreover, the fluorescence recovery, accompanied by the dissolution of MnO_2 nanosheets, can be used as a reporting signal for monitoring the transmission capacity.

Upconversion nanocompounds loaded with MnO_2 to replenish oxygen and increase PDT selectivity Under the effect of upconversion nanocompounds loaded with MnO_2, NIR light can be turned to ultraviolet (UV)/visible light with a broad emission spectrum; therefore, MnO_2-loaded upconversion nanocompounds can also be applied as powerful tools to activate various PSs. Meanwhile, MnO_2 can be decomposed in vivo to produce oxygen and further enhance PDT. As a result, NIR light-mediated upconversion nanocompounds, especially lanthanum-doped upconversion nanocrystals (UCNs) combined with MnO_2, have been systematically investigated to effectively induce cell extirpation.

Xing's group[52] demonstrated the successful establishment of PS-loaded UCN nanoconjugates (PUNs) that can enhance the effectiveness of PDT by reducing the population of tumor-associated macrophages (TAMs) and hypoxia. PUNs can be prepared by combining MnO_2 nanosheets with hyaluronic acid (HA) biopolymers (Fig. 10). When subjected to the acidic tumor microenvironment with excessive H_2O_2, MnO_2 nanosheets can be degraded and produce a large amount of oxygen, which can greatly improve the efficiency of oxygen-dependent PDT. Moreover, by transitioning NIR light to UV/visible light, PUNs can also offer a high degree of tissue penetration and help solve the safety problems involved in conventional PDT techniques. In addition, due to the existence of biologically stimulated HA, PUNs can drastically decrease the tumor recurrence rate by reprogramming the propagation of tumor-promoting M2 TAMs into tumor-unfavorable M1 macrophages. This strategy provides an excellent opportunity for enhanced cell ablation in NIR-mediated PDT therapy by weakening the hypoxic tumor microenvironment and therefore inspires new strategies for immunotherapy that can prevent tumor recurrence in the later stage of PDT.

In addition, mesoporous silica nanospheres incorporating fine CaF_2:Yb and Er upconversion nanocrystals were synthesized by the thermal decomposition method by Gu et al.[53]. Then, a new nano-PDT platform was obtained by coating the nanospheres with a thin layer of manganese dioxide and loading the PS Ce6. In the composite nanoparticles, Mn^{2+} ions doped in the CaF_2 crystal lattice effectively enhanced the red upconversion luminescence triggered by NIR light, which stimulated the adsorption of Ce6 by resonance energy transfer, thus improving the photodynamic phenomena. At the same time, the MnO_2 coating regulated the hypoxic microenvironment of tumors by the in situ generation of O_2 through reacting with endogenous H_2O_2 of tumors. These two mechanisms play important roles in the treatment of NIR-triggered photodynamic tumors. After Ce6 loading, the nanoparticles showed good stability in physiological solutions (including ultrapure water, phosphate-buffered saline, fetal bovine serum, and cell culture medium (RPMI-1640) containing 10% serum) without any agglomeration. More importantly, the results of in vivo experiments showed that the tumor shrank significantly under NIR light irradiation and remained small for 14 days without recurrence.

UCNPs loaded with MnO_2 based on this unique material design strategy not only have the anticancer prospects shown above but also offer guiding significance for the development of other types of functional nanostructures.

Other metal oxide nanomaterials Lan et al.[54] developed novel nano metal–organic framework-based metal oxide nanoparticles by using 5,10,15,20-tetra(*p*-benzoic acid)

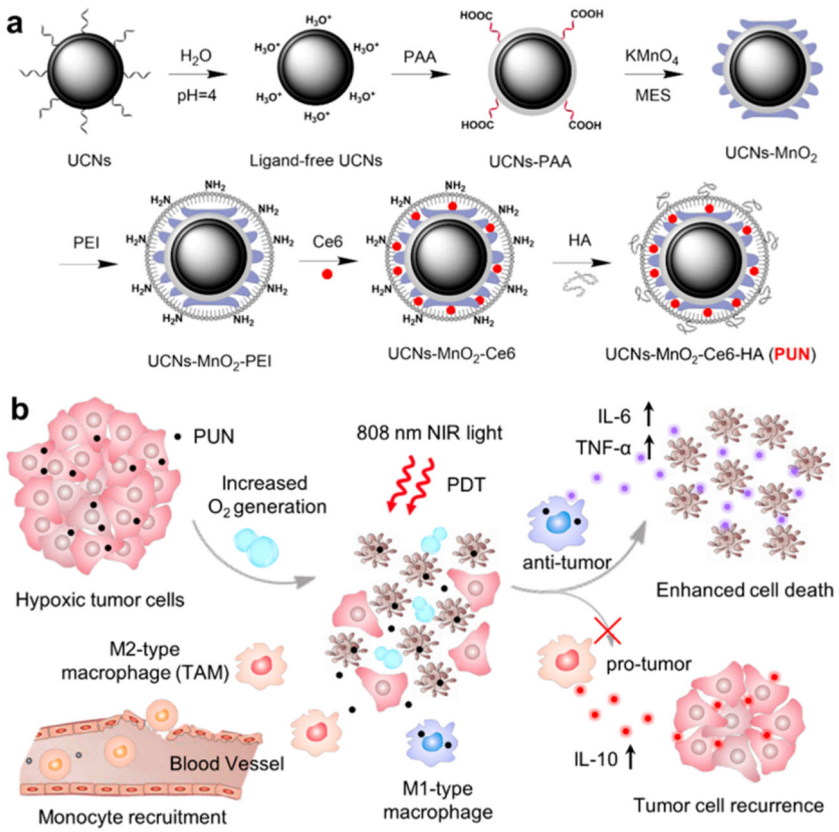

Fig. 10 Establishment of PS-loaded UCN nanoconjugates (PUNs) that can enhance PDT effect. a Schematics of the preparation of PUNs. **b** Schematic illustration of the enhanced PDT effect of PUNs by reducing the population of tumor-associated macrophages and hypoxia. Copyright 2018, American Chemical Society (ref. [52]).

porphyrin (TBP) ligands and Fe_3O clusters to form Fe-TBP, as illustrated schematically in Fig. 11. O_2 was generated by the Fenton-like reaction of Fe_3O clusters and then converted into cytotoxic singlet oxygen ($^1O_2$) by photostimulated porphyrin. PDT mediated by Fe-TBP can trigger a systemic antitumor response to improve alpha-PD-L1 ICB (immune checkpoint blocker), resulting in the disappearance of microscopic effects in treating primary and untreated distant tumors. Treatment with Fe-TBP plus alpha-PD-L1 can induce the proliferation of $CD4^+$ and $CD8^+$ T cells, which infiltrate distant tumors to induce exfoliation. In a mouse model of colorectal cancer, Fe-TBP-mediated PDT significantly improved the therapeutic effect of alpha-PD-L1. A sustained abscopal effect was induced, both the primary tumor under the treatment and the untreated distant tumor regressed >90%. Moreover, ICP-MS analysis showed that Fe-TBP mostly gathered at the tumor site after 4 h of incubation and was cleared within 10 days, and no dark regions indicating toxicity of Fe-TBP were observed. This study proposes a new strategy combining enhanced PDT with immune therapy to induce systemic antitumor therapy.

Moreover, due to the spontaneous cycling of cerium dioxide (CeO_2) between Ce^{3+} and Ce^{4+} in redox reactions, CeO_2 can react with high levels of endogenous H_2O_2 in tumor cells and simultaneously generate H_2O and O_2. Therefore, CeO_2 can be used as an optional O_2-evolving agent to enhance the efficacy of PDT. Zeng et al.[55] developed a core–shell Bi_2S_3@Ce6–CeO_2 nanocomposite. Bi_2S_3 showed good photothermal, photoacoustic, and computed X-ray tomography (CT) imaging performance, and the PS Ce6, which has good photodynamic effects, was adsorbed on the surface of Bi_2S_3. Finally, CeO_2, an O_2-evolving agent, was coated on the Bi_2S_3@Ce6 surface to provide an in situ oxygen supply. The biocompatibility of Bi_2S_3@Ce6–CeO_2 was evaluated by the MTT method, and the results showed that at concentrations of 12.5–200 μg/mL, 4T1 cells had a survival rate of more than 95% within 24 h, even at the maximum concentration of 200 μg/mL. The survival rate at 48 h also exceeded 90%. Similarly, Bi_2S_3@Ce6–CeO_2 showed consistently low toxicity in mouse embryonic fibroblast NIH 3T3 cells. Moreover, the results of in vivo treatment showed that the tumor volume of the mice in

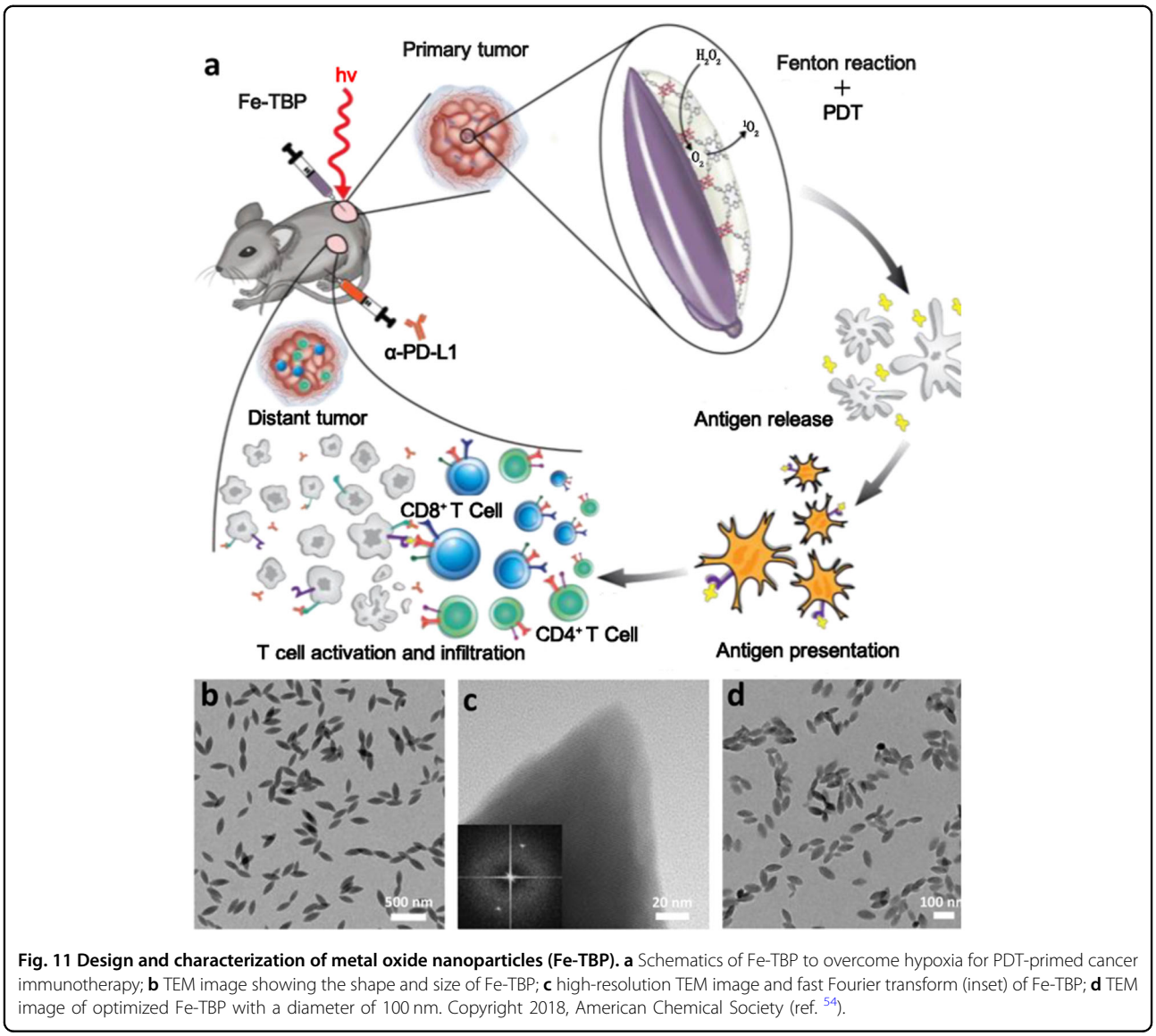

Fig. 11 Design and characterization of metal oxide nanoparticles (Fe-TBP). a Schematics of Fe-TBP to overcome hypoxia for PDT-primed cancer immunotherapy; **b** TEM image showing the shape and size of Fe-TBP; **c** high-resolution TEM image and fast Fourier transform (inset) of Fe-TBP; **d** TEM image of optimized Fe-TBP with a diameter of 100 nm. Copyright 2018, American Chemical Society (ref. [54]).

the Bi_2S_3@Ce6–CeO_2 group was close to zero, and the CD31 and Ki67 immunohistochemical results also showed significant damage to the microvessels of CD31-positive tumors and inhibited proliferation of positive cells. Multifunctional nanomaterials that combine photodynamic/photothermal/oxygen supply properties have shown improved tumor therapy efficacy both in vitro and in vivo.

Catalase-active material

Catalases capable of triggering the decomposition of H_2O_2 into water and oxygen are enriched in malignant tumor cells, with concentrations higher than those in healthy cells, and are closely related to the progression and proliferation of tumors. Such materials can also be used as an oxygen source to trigger PDT[56–59]. Based on this understanding, the concept that catalase-combined PS can enhance PDT efficiency by the synergistic promotion of in situ oxygen production in tumor tissues has been proposed and demonstrated.

For example, gold nanoclusters (AuNCs) have been widely used as materials with catalase activity in recent years[60,61]. Nanomaterial-based enzymes can be used as artificial catalases with controllable release to use catalase-like activities to catalyze the transformation of intratumoral H_2O_2 into O_2 to alleviate tumor hypoxia. Dan et al.[61] reported the use of ultrasmall AuNCs-ICG as nanozymes with theranostic features, efficient renal clearance, and superior catalase-like activity to modulate tumor hypoxia and enhance PDT and radioisotope tracer (RT) (Fig. 12). AuNCS effectively decompose a large

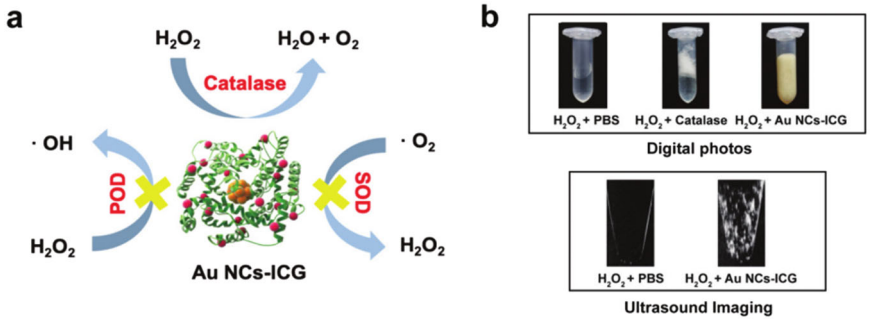

Fig. 12 Ultrasmal Au NCs-ICG served as nanozymes to modulate tumor hypoxia and enhance PDT. a Schematic illustration of the mechanism of AuNCs-ICG. **b** Digital photos and ultrasound images of H_2O_2 under different conditions. Copyright 2019, Royal Society of Chemistry (ref. [61]).

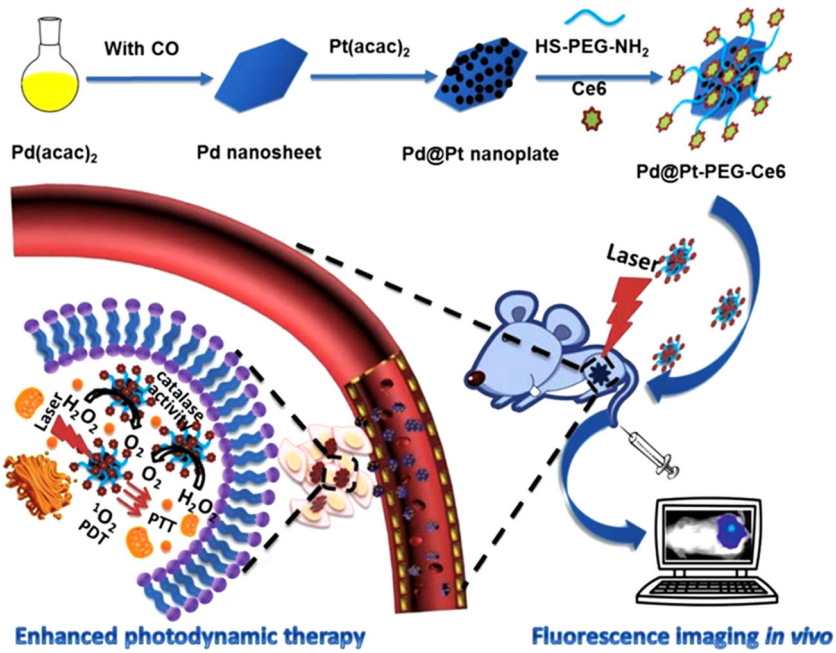

Fig. 13 An overview illustrating the preparation and application of Pd@Pt-PEG-Ce6. Copyright 2018, Wiley (ref. [62]).

amount of H_2O_2 in the tumor to produce oxygen, thus improving the naturally hypoxic tumor microenvironment and enhancing conventional PDT and RT efficacy.

Moreover, taking advantage of Pt's catalase activity to change H_2O_2 into oxygen, Wei et al.[62] designed novel two-dimensional PdS-based nanomaterials with good biocompatibility, good near-infrared absorption characteristics, and high tumor enrichment ability, which show great promise in the diagnosis and treatment of tumors. In particular, Pd@Pt-PEG-Ce6 nanocomposites were designed by using Pd–Pt two-dimensional palladium nanocomposites as carriers of PSs, as shown in Fig. 13. Pd@Pt-PEG-Ce6 can effectively deliver PS to tumor cells and decompose endogenous H_2O_2 to facilitate oxygen generation, thus significantly enhancing the efficacy of PDT. Moreover, the PDT efficacy of Pd@Pt-PEG-CE6 can also be improved by the mild photothermal effect of Pd:Pt nanoplates.

In addition, the combination of catalase and a PS to achieve a better PDT effect has been investigated. Hu's group[58] developed a new type of oxygen self-sufficient PDT platform by coloading with catalase and MB to construct zeolite-catalase-MB nanocapsules (ZCM nanocapsules), as illustrated by the SEM, TEM, and HRTEM images in Fig. 14. The prepared ZCM nanocapsules showed 90% relative activity compared to equivalent free catalase. Under real-time ultrasound imaging guidance, ZCM nanocapsules can be precisely implanted into the tumor area. Since they can decompose endogenous H_2O_2 in a sustained manner and provide in situ O_2 generation,

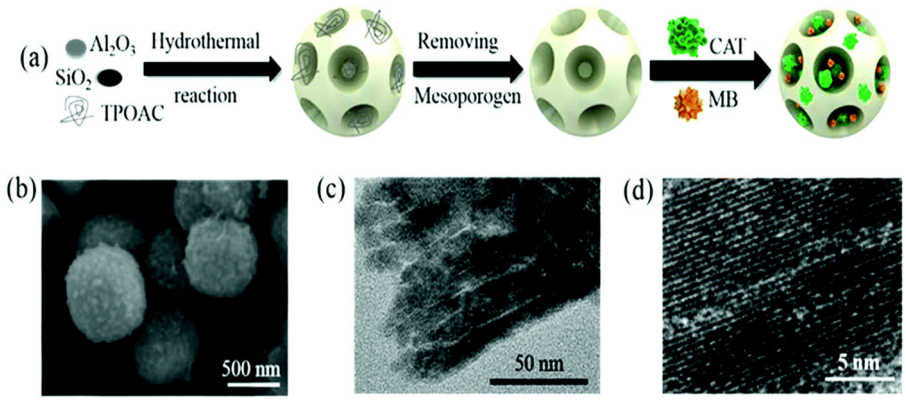

Fig. 14 Design and characterization of ZCM nanocapsules. a Schematics of the fabrication process of the ZCM nanocapsules; **b** SEM; **c** TEM; and **d** HRTEM images of the prepared ZCM nanocapsules. Copyright 2018, Royal Society of Chemistry (ref. [58]).

the ZCM nanocapsules can effectively improve hypoxia and enhance intratumoral ultrasound contrast. Moreover, the incorporated MB can prevent the rapid leaching of the PS and contribute to its sustained release of PS at tumor site. In vitro results demonstrated that local PC cells can be completely killed upon near-infrared laser irradiation, and no therapy-induced side effects or tumor recurrence were observed. As described above, the use of catalase-active materials in combination with PSs and the formation of new processing systems through reasonable design strategies will help overcome the challenges in PDT and improve its efficacy.

Water-splitting materials

Current strategies for oxygen supplementation typically involve the use of biological oxygen-producing materials such as MnO_2 and catalase-like materials, but their O_2 yield may be limited by intracellular restricted H_2O_2 concentrations. In nature, plants produce oxygen efficiently from abundant H_2O through photosynthesis. Inspired by this phenomenon, water-splitting materials, such as nanocomposites based on inorganic, organic, macromolecular, or hybrid materials, have been developed to produce H_2 and O_2[63–65]. As the most abundant compound in organisms, water can provide almost unlimited O_2 production compared with other oxygen-producing materials. At present, the main water-splitting materials used to alleviate PDT hypoxia therapy are calcium peroxide (CaO_2) nanoparticles, carbon nitride (C_3N_4) nanocomposites, and TiO_2 nanotubes.

Calcium peroxide (CaO_2) nanoparticles CaO_2, a safe water-splitting material with high biocompatibility, rapid cell metabolism, and efficient O_2 production, is considered to be a promising material to regulate solid tumor hypoxia and improve PDT efficiency[66,67]. It can generate a large amount of O_2 upon coming into contact with water to improve PDT efficacy. Typical CaO_2-based oxygen-producing biomaterials are mainly fabricated by combining CaO_2 with hydrophobic polymers.

For instance, Liu et al.[68] synthesized the liposome-based nanoparticle LipoMB/CaO_2 with oxygen self-enrichment properties (Fig. 15). Under laser irradiation, the singlet oxygen produced by the PS MB can induce lipid peroxidation and destroy the liposome structure, further exposing CaO_2, expanding the contact area between CaO_2 and H_2O and producing a large amount of oxygen to alleviate hypoxia. In vivo and in vitro experiments have demonstrated that LipoMB/CaO_2 shows superior oxygen production capability with an enhanced PDT effect that can effectively alleviate hypoxia in tumors.

Carbon nitride (C_3N_4) nanocomposites Among water-decomposing materials, C_3N_4 has attracted much attention due to its relatively narrow band gap (2.7 eV) and strong reduction ability. Water splitting by C_3N_4 can be triggered under high-penetration red light (>600 nm), making it suitable for in vivo therapy. Moreover, since C_3N_4 is not doped with metal elements, it has high biocompatibility, good stability, and nontoxicity, and can be used in the biomedical field[69–73].

For example, Zhang's group[74] designed an intelligent nanoreactor R-NCNP with a combined water-splitting effect and multimodal imaging function (Fig. 16). This nanocomposite has a mesoporous C_3N_4 layer coated on the core–shell structure of nitrogen-doped graphene quantum dot (N-GQD)@hollow mesoporous silica nanosphere and then bound P-PEG-RGD amphiphilic polymers to achieve targeted delivery, resulting in the nanoreactor designated R-NCNP. Upon 630 nm laser irradiation, the PSs are activated to produce singlet oxygen, while H_2O molecules are transformed into O_2 to increase the tumor oxygen content through C_3N_4-mediated water-splitting. In addition, N-GQDs endow

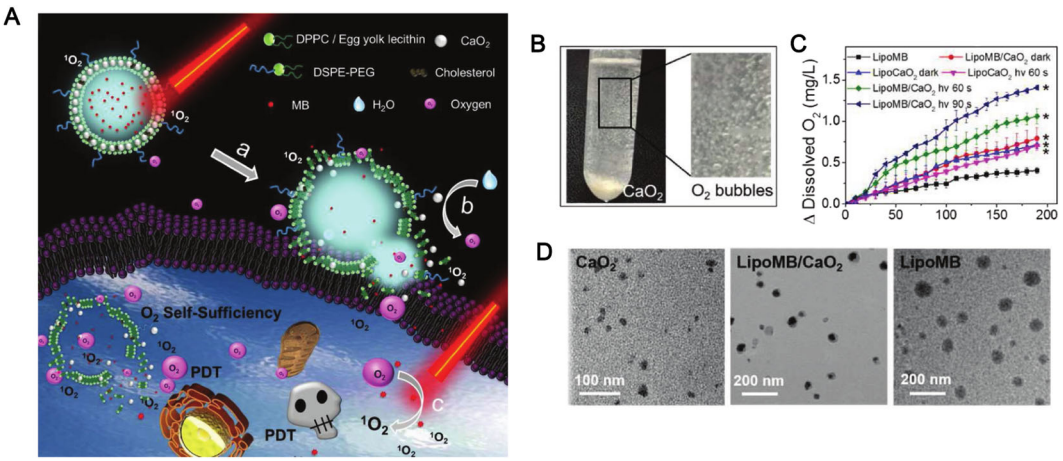

Fig. 15 The mechanism and characterization LipoMB/CaO_2. a Structure illustration of LipoMB/CaO_2 nanoparticles for alleviating anoxic environments. **b** Image of O_2 bubbles generated by CaO_2 solids reacting with H_2O. **c** Δ Dissolved O_2 in LipoCaO$_2$, LipoMB/CaO_2, and LipoMB solutions with or without laser irradiation. **d** TEM image of CaO_2, LipoMB/CaO_2, and LipoMB nanoparticles. Copyright 2017, Wiley (ref. [68]).

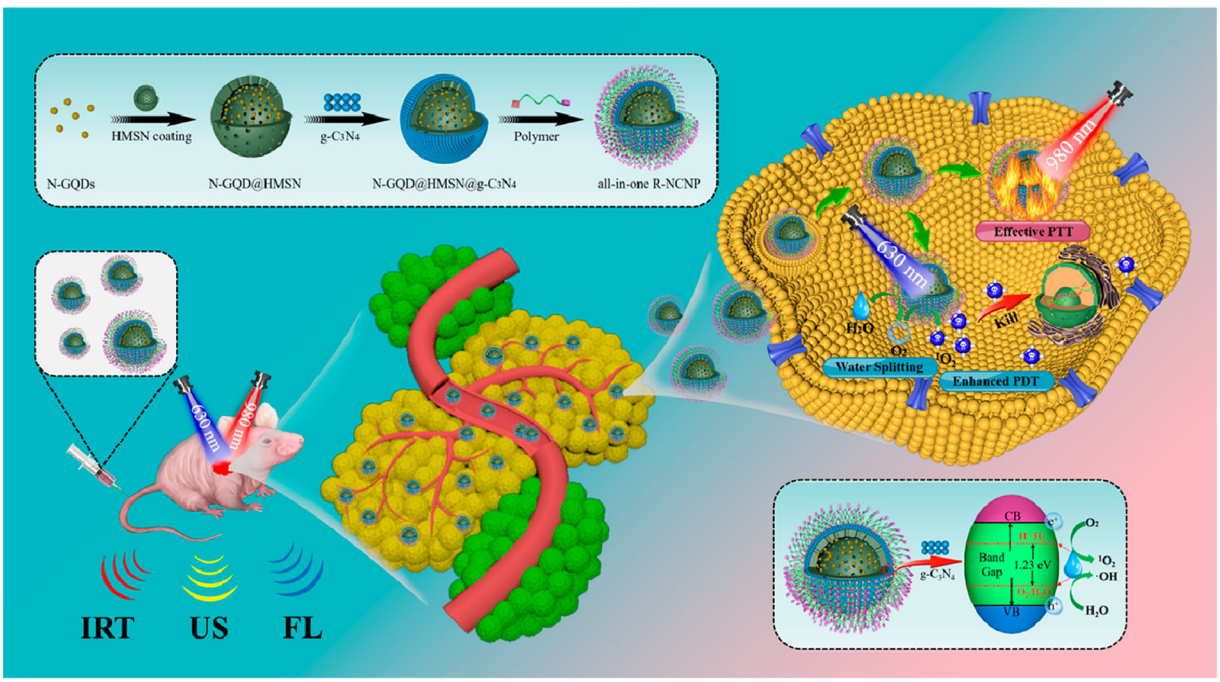

Fig. 16 Schematic illustration of the synthesis steps and the PDT/PTT therapeutic mechanism based on smart R-NCNP nanocomposites. Copyright 2020, American Chemical Society (ref. [74]).

R-NCNP with both PTT/PDT and imaging capabilities. Experimental results show that R-NCNP can enhance the efficacy of PDT by alleviating hypoxia and assist with multimodal imaging for a good combination of diagnosis and treatment. Moreover, the distribution in the body showed only a weak fluorescent signal in the liver, possibly caused by phagocytosis of the nanoparticles by mononuclear phagocytes. In addition, a moderate accumulation of fluorescence was detected in the kidney tissue, indicating that the nanoparticles were excreted and eliminated from the kidney.

TiO_2 nanotubes TiO_2 materials have attracted extensive attention in the field of water-splitting materials due to their adjustable band gap, excellent photostability, high catalytic activity, low toxicity, and low cost[75,76]. They can

provide large internal and external surface areas to improve the light absorption intensity and facilitate further modification. They can be used in combination with carbon nanodots (CDots) for PDT treatment via water-splitting processes:

$$2H_2O \rightarrow H_2O_2 + H_2; \quad (3)$$

$$2H_2O_2 \rightarrow 2H_2O + O_2. \quad (4)$$

Yang et al.[77] designed carbon nanodot-modified TiO_2 nanotubes (CDots/TiO_2 NTS) to release oxygen and reactive oxygen species simultaneously in an anoxic environment. Under laser irradiation, the CDots/TiO_2 PS will produce a large amount of singlet oxygen through an upconversion process to induce apoptosis or necrosis and supply a large amount of oxygen through continuous water splitting to improve the efficacy of PDT. Experimental results in vivo and in vitro show that CDots/TiO_2 NTS have good PDT effects, which makes them an excellent photosensitive material with great potential for application in the biomedical field.

Other strategies involving regulating tumor microenvironments and multimodal therapy including PDT

Improving blood perfusion in tumors

With the rapid growth of solid tumors, the formation of a neovascular network lags behind cell proliferation, and the construction of a new microvascular network is irregular. The abnormal vascular network has temporary closure or "blind ends", which a decrease of tumor blood perfusion and oxygen partial pressure (pO_2) in the microenvironment, making it difficult for the tumor to obtain an adequate O_2 supply to meet its metabolic needs, resulting in tumor hypoxia and reducing the therapeutic effect of PDT[78–81]. Therefore, improving blood flow perfusion by improving vascular conditions in tumors is a good approach to increasing oxygen content. It is mainly achieved by improving tumor hemodynamics via photothermal therapy (PTT) and regulating tumor microvessel structure using chemotherapeutic drugs.

Improving tumor hemodynamics

Tumor hypoxia is largely related to disordered and chaotic tumor blood flow, so improving blood flow has become an effective way to increase tumor O_2 concentration. Many studies have shown that increasing local temperature by mild heating can effectively increase tumor blood flow and increase oxygen content in solid tumors[82,83]. Therefore, the combination of PDT and PTT is often used to treat cancer cells, as PTT can not only convert light energy into heat energy under the irradiation of an external light source to kill cancer cells but also be administered as a mild photothermal pretreatment to improve blood flow in solid tumors.

Our group[84] designed a dual oxygenated nanoparticle MnO_2@chitosan-CyI (MCC) for enhanced phototherapy, in which the PS CyI is a near-infrared dye with both PDT and PTT effects. When exposed to near-infrared radiation, the increase in tissue temperature caused by the photothermal effect accelerates blood flow and effectively alleviates tumor hypoxia. Moreover, MnO_2 can not only reduce the level of GSH but also act as an efficient in situ oxygen generator, thus further increasing the production of ROS. This MCC nanosystem shows great promise as an intelligent and versatile nanotherapy platform that can improve the tumor microenvironment under hypoxia to obtain better therapeutic effects of PDT/PTT.

Regulation of tumor microvessel structure

In addition to using photothermal effects to increase blood flow velocity within solid tumors, chemotherapeutic drugs have recently been used to regulate the disordered microvascular structure of tumors (e.g., gemcitabine, cyclophosphamide, and cisplatin) to restore the physiological perfusion and oxygenation of tumor vessels more efficiently[85–87]. For example, Shen et al.[88] found that thalidomide (Thal) can correct the imbalance between proangiogenic factors and antiangiogenic factors, resulting in decreased leakage of tumor vessels and increased thickness of blood vessels as well as tumor perfusion (Fig. 17). Finally, the tumor vascular system was normalized and tumor oxygenation was increased. Thal, as a new candidate drug, can maximize the efficacy of PDT for solid tumors if combined with a PS.

Targeting mitochondria in tumors

A lack of sustained alleviation of hypoxia in solid tumors is one of the major problems for in situ oxygen-producing nanomaterials, since the uninterrupted high respiration in tumors consumes oxygen through mitochondria. As an indispensable organelle responsible for cell respiration, mitochondria may aggravate tumor hypoxia and limit the efficacy of PDT[89,90]. Hence, it is feasible to design nanocomposites that can selectively inhibit mitochondrial activity and produce O_2 sustainably in hypoxic tumors.

For example, Yang et al.[91] constructed photodynamic Mn_3O_4@MSNs@IR780 nanoparticles with sustainable hypoxia mitigation capabilities (Fig. 18). The alleviation of hypoxia is achieved through intratumor H_2O_2 catalysis and targeting mitochondria to inhibit respiration. These Mn_3O_4 nanoparticles responded to the H_2O_2-enriched tumor microenvironment by decomposing and catalyzing H_2O_2 to produce O_2. Subsequently, IR780 was released and activated and spontaneously targeted mitochondria due to its natural mitochondrial affinity. Under laser

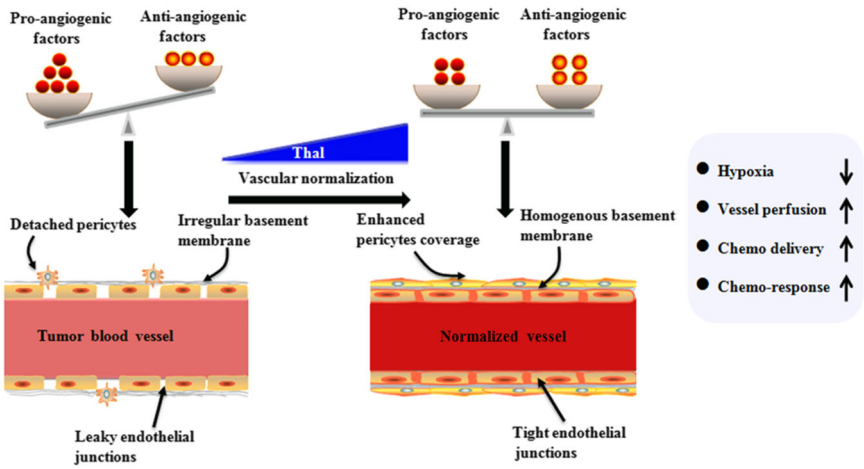

Fig. 17 Schematic diagram depicting changes in the tumor vascular system caused by Thal-induced vascular normalization in solid tumors. Copyright 2019, BioMed Central (ref. [88]).

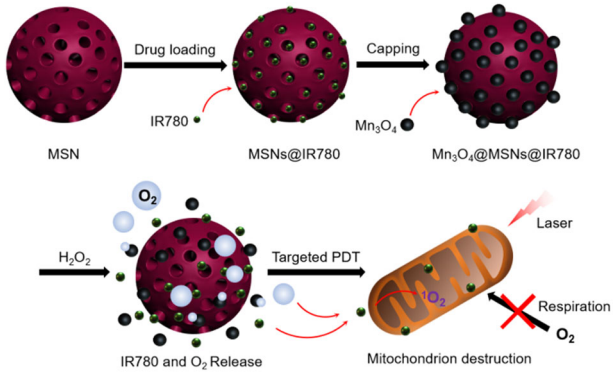

Fig. 18 Schematic diagram of the synthetic processes of Mn_3O_4@MSNs@IR780. H_2O_2 triggered the release of IR780 and O_2, and mitochondria targeted PDT. Copyright 2019, Ivyspring International Publisher (ref. [91]).

irradiation, Mn_3O_4@esoporous silica nanomaterials (MSNs)@IR780 can destroy mitochondria and inhibit cell respiration, which can alleviate the persistent hypoxia of tumor tissue, thus improving the therapeutic effect of PDT. In vitro experiments showed that Mn_3O_4@MSNs@IR780 can continuously alleviate tumor hypoxia and provide a new way to overcome sustainable hypoxia.

Downregulating HIF-1 expression in tumors

The high expression of hypoxia-inducible factor (HIF-1α) is one of the key barriers to PDT treatment. Although current in situ oxygen supply strategies can alleviate tumor hypoxia to some extent, the non-sustainable supply of O_2 offered by these strategies can induce only moderate HIF-1α degradation, and the residual HIF-1α will still adversely affect the PDT effect. Using effective HIF-1α inhibition in hypoxic tumors is a feasible way to achieve adequate tumor oxygenation to enhance PDT efficacy. Inspired by HIF-1 intracellular signaling pathways, researchers have been working on the precise blocking of HIF-1α by small molecular inhibitors in recent years[92,93].

Liu et al.[94] utilized rapamycin (RAP) as an upstream activator of HIF-1 and mammalian rapamycin targeting gene (mTOR) inhibitor in cancer cells, whose inhibition of mTOR leads to HIF-1α expression and HIF-1 transcription-dependent blockade. As illustrated in Fig. 19, an efficient core–shell nanosystem was designed to alleviate hypoxia and improve PDT efficacy through simultaneous oxygenation and HIF-1α inhibition. The PSs Ce6 and RAP formed dual-drug nanopores through self-assembly and were then loaded with catalase. Catalase, as an oxygen provider, catalyzes H_2O_2 decomposition into O_2 and leads to the sustained release of RAP to downregulate HIF-1α expression, thus achieving in situ oxygen generation and HIF-1α inhibition in tumor tissues, together relieving PDT pressure on hypoxia.

PDT-activated hypoxia-amplified bioreductive therapy

In recent years, the application of hypoxia-reactive anticancer drugs combined with PDT under hypoxic conditions has aroused great interest. Unlike other strategies focused on alleviating hypoxia in tumors, this new approach takes advantage of the lack of oxygen in tumors. In addition, PDT-induced oxygen consumption can further enhance the role of hypoxia-activated drugs. Recent studies have demonstrated the feasibility and effectiveness of this strategy, in which the combined delivery of PS and prodrugs is achieved by nanoparticles, such as silica-shell nanoparticles or liposomes[95–98].

Hypoxic response drugs usually produce highly cytotoxic substances under hypoxic conditions, and their

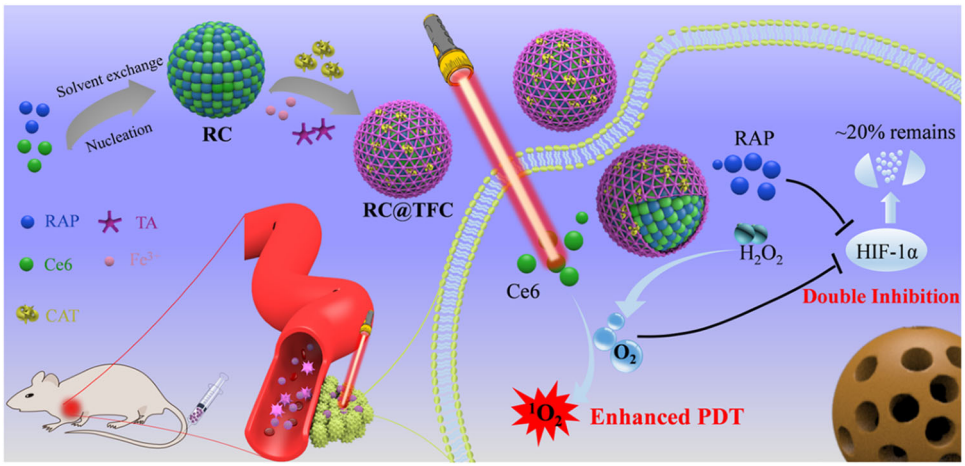

Fig. 19 Schematic illustration of a core–shell nanocomposite for enhancing PDT by simultaneous in situ oxygenation and HIF-1α inhibition. Copyright 2019, American Chemical Society (ref. [94]).

cytotoxic activity can be triggered when combined with hypoxic induction therapy. The current combination of PDT with hypoxia-responsive drugs mainly involves telapamide (TPZ), TH-302, PR-104A, and benzoanthraquinone (AQ4N), which produce sufficient hypoxia in tumors by cotransporting with PS molecules and show strong cytotoxicity in the hypoxic microenvironment. Although this approach is rarely used in the field of PDT, its anticancer potential is certainly worth further exploration and confirmation.

Liu et al.[99] designed double-layer silica-shell UCNPs, which can transfer the PS and bioreductive precursor drug TPZ together to achieve synergistic cancer treatment. UC-PDT was used to induce the cytotoxicity of active TPZ and produced a large amount of ROS. Compared with UC-PDT, TPZ UC/PS can significantly inhibit the growth of tumors, suggesting that TPZ exhibits a significant increase in cytotoxicity during PDT-induced hypoxia and has a profound impact on the therapeutic effect. This NIR-induced intratumoral hypoxia is sufficient to enhance hypoxia-induced bioreduction therapy, demonstrating an efficient synergistic approach to cancer treatment.

Conclusions and outlooks

Because of its minimal invasiveness, high feasibility, and enhanced efficiency, PDT has made tremendous progress in anticancer therapy. The latest advances in oxygen supplementation nanoparticles have opened up promising perspectives to develop new PDT systems and provide multiple opportunities to circumvent the current PDT paradigm. On the one hand, exogenous molecular oxygen can be captured by biological, bionic, or physical mechanisms and then transported to solid tumors with the help of nanocarriers. On the other hand, through PDT-dependent materials, PDT-in-dependent materials or other methods, oxygen can be generated in vivo to provide a continuous local oxygen supply to improve PDT efficiency. Both strategies have demonstrated their potential in improving the oxygen content of PDT.

In this review, we present strategies to improve PDT efficiency by focusing on hypoxia, a key challenge in PDT-mediated cancer therapy. However, it is worth noting that although a large number of studies investigated improving PDT efficiency by relieving hypoxia in the tumor microenvironment, increasing the singlet oxygen yield of the PS itself is also an important means to enhance the efficiency of PDT. For example, we found that the heavy metal atom iodine can be modified in ICG PSs by the heavy atom effect and can significantly improve the singlet oxygen yield[100]. If such PSs are combined with the oxygen supplements described above, better PDT effects are expected. In addition, for clinical applications, PDT needs to meet many specific requirements, including biocompatibility and biodegradability. For example, when manganese dioxide nanosheets are used to produce oxygen, their degradation needs to be carefully evaluated in vivo. With these challenges seriously considered and addressed, overcoming tumor hypoxia in the use of PDT will become a powerful and versatile strategy for complicated cancer therapy.

Conflict of interest

The authors declare no competing interests.

Publisher's note

Received: 26 August 2020 Revised: 21 January 2021 Accepted: 29 January 2021.
Published online: 30 April 2021

References

1. Chi, J. et al. Targeted nanocarriers based on iodinated-cyanine dyes as immunomodulators for synergistic phototherapy. *Nanoscale* **12**, 11008–11025 (2020).
2. Agostinis, P. et al. Photodynamic therapy of cancer: an update. *CA Cancer J. Clin.* **61**, 4 (2015).
3. Wang, Moriyama & Bagnato Photodynamic therapy induced vascular damage: an overview of experimental PDT. *Laser Phys. Lett.* **10**, e023001 (2013).
4. Kimakova, P. et al. Photoactivated hypericin increases the expression of SOD-2 and makes MCF-7 cells resistant to photodynamic therapy. *Biomed. Pharmacother.* **85**, 749–755 (2017).
5. Dang, J., He, H., Chen, D. & Yin, L. Manipulating tumor hypoxia toward enhanced photodynamic therapy (PDT). *Biomater. Sci.* **5**, 1500–1511 (2017).
6. Gao, Z. et al. Biomimetic platinum nanozyme immobilized on 2D metal-organic frameworks for mitochondria-targeting and oxygen self-supply photodynamic therapy. *ACS Appl. Mater. Interfaces* **12**, 1963–1972 (2019).
7. Sun, X., Ni, N., Ma, Y., Wang, Y. & Leong, D. Retooling cancer nanotherapeutics' entry into tumors to alleviate tumoral hypoxia. *Small* **16**, e2003000 (2020).
8. Wu, J. et al. A tumor microenvironment-responsive biodegradable mesoporous nanosystem for anti-inflammation and cancer theranostics. *Adv. Healthc. Mater.* **9**, e1901307 (2019).
9. Azuma, H., Fujihara, M. & Sakai, H. Biocompatibility of HbV: liposome-encapsulated hemoglobin molecules-liposome effects on immune function. *J. Funct. Biomater.* **8**, 24 (2017).
10. Fleming, I. N. et al. Imaging tumour hypoxia with positron emission tomography. *Br. J. Cancer* **112**, 238–250 (2015).
11. Li, T., Jing, X. & Huang, Y. Polymer/hemoglobin assemblies: biodegradable oxygen carriers for artificial red blood cells. *Macromol. Biosci.* **11**, 865–875 (2011).
12. Wang, S. et al. Synthesis of hemoglobin conjugated polymeric micelle: a ZnPc carrier with oxygen self-compensating ability for photodynamic therapy. *Biomacromolecules* **16**, 2693–2700 (2015).
13. Li, J. et al. An assembled nanocomplex for improving both therapeutic efficiency and treatment depth in photodynamic therapy. *Angew. Chem. Int. Ed.* **57**, 7759 (2018).
14. Liu, W. L. et al. Aggressive man-made red blood cells for hypoxia-resistant photodynamic therapy. *Adv. Mater.* **30**, e1802006 (2018).
15. Yu, B. et al. Inhaled nitric oxide enables artificial blood transfusion without hypertension. *Circulation* **117**, 1982–1990 (2008).
16. Chen, Z. et al. Bioinspired hybrid protein oxygen nanocarrier amplified photodynamic therapy for eliciting anti-tumor immunity and abscopal effect. *ACS Nano.* **12**, 8633–8645 (2018).
17. Ong, Y. H. et al. Determination of optical properties, drug concentration and tissue oxygenation in human pleural tissue before and after Photofrin-mediated photodynamic therapy. *Proc. SPIE Int. Soc. Opt. Eng.* **10476**, 10476Y (2018).
18. Yang, J. et al. Hypoxic tumor therapy by hemoglobin-mediated drug delivery and reversal of hypoxia-induced chemoresistance. *Biomaterials* **182**, 145 (2018).
19. Luo, Z. et al. Self-monitoring artificial red cells with sufficient oxygen supply for enhanced photodynamic therapy. *Sci. Rep.* **6**, 23393 (2016).
20. Riess, J. G. Perfluorocarbon-based oxygen delivery. *Artif. Cells Blood Substit. Immobil. Biotechnol.* **34**, 567–580 (2006).
21. Wilhelm, E. & Battino, R. Thermodynamic functions of the solubilities of gases in liquids at 25. deg. *Chem. Rev.* **73**, 1–9 (1973).
22. Li, N. et al. Perfluorocarbon nanocapsules improve hypoxic microenvironment for the tumor ultrasound diagnosis and photodynamic therapy. *J. Biomed. Nanotechnol.* **14**, 2162–2171 (2018).
23. Day, R., Estabrook, D., Logan, J. & Sletten, E. Fluorous photosensitizers enhance photodynamic therapy with perfluorocarbon nanoemulsions. *Chem. Commun.* **53**, 13043 (2017).
24. Sheng, D. et al. Perfluorooctyl bromide & indocyanine green co-loaded nanoliposomes for enhanced multimodal imaging-guided phototherapy. *Biomaterials* **165**, 1 (2018).
25. Sun, Y. et al. Recent progress of hypoxia-modulated multifunctional nanomedicines to enhance photodynamic therapy: opportunities, challenges, and future development. *Acta Pharm. Sin. B* **10**, 1382–1396 (2018).
26. Ren, H. et al. Relighting photosensitizers by synergistic integration of albumin and perfluorocarbon for enhanced photodynamic therapy. *ACS Appl. Mater. Interfaces* **9**, 3463 (2017).
27. Yu, M. et al. Perfluorohexane-cored nanodroplets for stimulations-responsive ultrasonography and O_2-potentiated photodynamic therapy. *Biomaterials* **175**, 61–71 (2018).
28. Song, X., Feng, L., Liang, C., Yang, K. & Liu, Z. Ultrasound triggered tumor oxygenation with oxygen-shuttle nanoperfluorocarbon to overcome hypoxia-associated resistance in cancer therapies. *Nano. Lett.* **16**, 1645 (2016).
29. Jia, X. et al. Perfluoropentane-encapsulated hollow mesoporous prussian blue nanocubes for activated ultrasound imaging and photothermal therapy of cancer. *ACS Appl. Mater. Interfaces* **7**, 4579–4588 (2015).
30. Chan, X. et al. Extensive submacular haemorrhage in polypoidal choroidal vasculopathy managed by sequential gas displacement and photodynamic therapy: a pilot study of one-year follow up. *Clin. Exp. Ophthalmol.* **33**, 611–618 (2005).
31. Cheng, Y. et al. Perfluorocarbon nanoparticles enhance reactive oxygen levels and tumour growth inhibition in photodynamic therapy. *Nat. Commun.* **6**, 8785 (2015).
32. Song, X. et al. Ultrasound triggered tumor oxygenation with oxygen-shuttle nanoperfluorocarbon to overcome hypoxia-associated resistance in cancer therapies. *Nano. Lett.* **16**, 6145–6153 (2016).
33. Mcewan, C. et al. Oxygen carrying microbubbles for enhanced sonodynamic therapy of hypoxic tumours. *J. Control Release* **203**, 51–56 (2015).
34. Song, R., Hu, D., Chung, H., Sheng, Z. & Yao, S. Lipid-polymer bilaminar oxygen nanobubbles for enhanced photodynamic therapy of cancer. *ACS Appl. Mater. Interfaces* **10**, 36805–36813 (2018).
35. Zhou, T., Xing, L., Fan, Y., Cui, P. & Jiang, H. Light triggered oxygen-affording engines for repeated hypoxia-resistant photodynamic therapy. *J. Control Release* **307**, 44–54 (2019).
36. Zhang, X. L. et al. Light-enhanced hypoxia-response of conjugated polymer nanocarrier for successive synergistic photodynamic and chemo-therapy. *ACS Appl. Mater. Interfaces* **10**, 21909 (2018).
37. Xu, S. et al. Oxygen and Pt(II) self-generating conjugate for synergistic photo-chemo therapy of hypoxic tumor. *Nat. Commun.* **9**, 2053 (2018).
38. Zeng, D. et al. Synergistic photothermal/photodynamic suppression of prostatic carcinoma by targeted biodegradable MnO_2 nanosheets. *Drug Deliv.* **26**, 661–672 (2019).
39. Tian, X., Cao, P., Zhang, H., Li, Y. & Yin, X. GSH-activated MRI-guided enhanced photodynamic and chemo-combination therapy with a MnO_2-coated porphyrin metal organic framework. *Chem. Commun.* **55**, 6241–6244 (2019).
40. Cao, Y. et al. Intelligent MnO_2/Cu^{2-} xS for multimode imaging diagnostic and advanced single-laser irradiated photothermal/photodynamic therapy. *ACS Appl. Mater. Interfaces* **10**, 17732–17741 (2018).
41. Wang, S. et al. MSOT/CT/MR imaging-guided and hypoxia-maneuvered oxygen self-supply radiotherapy based on one-pot MnO_2-$mSiO_2$@Au nanoparticles. *Nanoscale* **11**, 6270–6284 (2019).
42. Zhu, W. et al. Modulation of hypoxia in solid tumor microenvironment with MnO_2 nanoparticles to enhance photodynamic therapy. *Adv. Funct. Mater.* **56**, 5490 (2016).
43. Chu, C. et al. Tumor microenvironment-triggered supramolecular system as an in situ nanotheranostic generator for cancer phototherapy. *Adv. Mater.* **29**, e1605928 (2017).
44. Tao, Y. et al. Nano-graphene oxide-manganese dioxide nanocomposites for overcoming tumor hypoxia and enhancing cancer radioisotope therapy. *Nanoscale* **10**, 5114–5123 (2018).
45. Ji, C. et al. Self-production of oxygen system CaO_2/MnO_2@PDA-MB for the photodynamic therapy research and switch-control tumor cell imaging. *J. Biomed. Mater. Res. B.* **106**, 2544 (2018).
46. Meng, L. et al. Facile deposition of manganese dioxide to albumin-bound paclitaxel nanoparticles for modulation of hypoxic tumor microenvironment to improve chemoradiation therapy. *Mol. Pharm.* **15**, 447–457 (2018).
47. Jia, X. et al. Tumor microenvironment-responsive mesoporous MnO_2-coated upconversion nanoplatform for self-enhanced tumor theranostics. *Adv. Funct. Mater.* **28**, e1803804 (2018).
48. Kiesslich, T. et al. Differential effects of glucose deprivation on the cellular sensitivity towards photodynamic treatment-based production of reactive oxygen species and apoptosis-induction. *FEBS Lett.* **579**, 185–190 (2005).

49. He, D. et al. A sensitive turn-on fluorescent probe for intracellular imaging of glutathione using single-layer MnO_2 nanosheet-quenched fluorescent carbon quantum dots. *Chem. Commun.* **51**, 14764 (2015).
50. Sun, Y., Chen, H., Liu, G., Ma, L. & Wang, Z. The controllable growth of ultrathin MnO_2 on polydopamine nanospheres as a single nanoplatform for the MRI-guided synergistic therapy of tumors. *J. Mater. Chem. B.* **7**, 7152–7161 (2019).
51. Fan, H. et al. A smart photosensitizer–manganese dioxide nanosystem for enhanced photodynamic therapy by reducing glutathione levels in cancer cells. *Angew. Chem. Int. Ed.* **55**, 5611–5611 (2016).
52. Ai, X. et al. Enhanced cellular ablation by attenuating hypoxia status and reprogramming tumor-associated macrophages via NIR light-responsive upconversion nanocrystals. *Bioconjugate Chem.* **29**, 928–938 (2018).
53. Gu, T. et al. Upconversion composite nanoparticles for tumor hypoxia modulation and enhanced near-infrared-triggered photodynamic therapy. *ACS Appl. Mater. Interfaces* **10**, 15494–15503 (2018).
54. Lan, G. et al. Nanoscale metal-organic framework overcomes hypoxia for photodynamic therapy primed cancer immunotherapy. *J. Am. Chem. Soc.* **140**, 5670–5673 (2018).
55. Zeng, L. et al. A one-pot synthesis of multifunctional Bi_2S_3 nanoparticles and the construction of core–shell Bi_2S_3@Ce6–CeO_2 nanocomposites for NIR-triggered phototherapy. *J. Mater. Chem. B* **8**, 4093–4105 (2020).
56. Price, M., Terlecky, S. & Kessel, D. A role for hydrogen peroxide in the pro-apoptotic effectsof photodynamic therapy. *Photochem. Photobiol.* **85**, 1491–1496 (2009).
57. Cai, X. et al. Integrating in situ formation of nanozymes with three-dimensional dendritic mesoporous silica nanospheres for hypoxia-overcoming photodynamic therapy. *Nanoscale* **10**, 22937–22945 (2018).
58. Hu, D. et al. A catalase-loaded hierarchical zeolite as an implantable nanocapsule for ultrasound-guided oxygen self-sufficient photodynamic therapy against pancreatic cancer. *Nanoscale* **10**, 17283–17292 (2018).
59. Yao, C. et al. Near-infrared upconversion mesoporous cerium oxide hollow biophotocatalyst for concurrent pH-/H_2O_2-responsive O_2-evolving synergetic cancer therapy. *Adv. Mater.* **30**, e1704833 (2018).
60. Liu, C. et al. Self-supplying O_2 through the catalase-like activity of gold nanoclusters for photodynamic therapy against hypoxic cancer cells. *Small* **13**, 1700278 (2017).
61. Dan, Q. et al. Ultrasmall theranostic nanozymes to modulate tumor hypoxia for augmenting photodynamic therapy and radiotherapy. *Biomater. Sci.* **8**, 973–987 (2020).
62. Wei, J. et al. A novel theranostic nanoplatform based on Pd@Pt-PEG-Ce6 for enhanced photodynamic therapy by modulating tumor hypoxia microenvironment. *Adv. Funct. Mater.* **28**, e1706310 (2018).
63. Krüger, S. et al. Bombyx mori silk/titania/gold hybrid materials for photocatalytic water splitting: combining renewable raw materials with clean fuels. *Beilstein J. Nanotechnol.* **9**, 187–204 (2018).
64. Fu, C., Wu, X. & Yang, J. Material design for photocatalytic water splitting from a theoretical perspective. *Adv. Mater.* **30**, e1802106 (2018).
65. Perović, K. et al. Recent achievements in development of TiO_2-Based composite photocatalytic materials for solar driven water purification and water splitting. *Materials* **13**, 1338 (2020).
66. Liu, C. et al. An open source and reduce expenditure ROS generation strategy for chemodynamic/photodynamic synergistic therapy. *Nat. Commun.* **11**, 1735 (2020).
67. Ji, C. et al. Self-production of oxygen system CaO_2 /MnO_2@PDA-MB for the photodynamic therapy research and switch-control tumor cell imaging. *J. Biomed. Mater. Res. B.* **106**, 2544–2552 (2018).
68. Liu, L. et al. Dual-stage light amplified photodynamic therapy against hypoxic tumor based on an O_2 self-sufficient nanoplatform. *Small* **13**, 1701621 (2017).
69. Zheng, D. et al. Carbon-dot-decorated carbon nitride nanoparticles for enhanced photodynamic therapy against hypoxic tumor via water splitting. *ACS Nano* **10**, 8715–8722 (2016).
70. Feng, L. et al. Multifunctional UCNPs@$MnSiO_3$@g-C_3N_4 nanoplatform: improved ROS generation and reduced glutathione levels for highly efficient photodynamic therapy. *Biomater. Sci.* **5**, 2456–2467 (2017).
71. Wan, H., Zhang, Y., Zhang, W. & Zou, H. Robust two-photon visualized nanocarrier with dual targeting ability for controlled chemo-photodynamic synergistic treatment of cancer. *ACS Appl. Mater. Interfaces* **7**, 9608–9618 (2015).
72. Yang, D. et al. Multifunctional theranostics for dual-modal photodynamic synergistic therapy via stepwise water splitting. *ACS Appl. Mater. Interfaces* **9**, 6829–6838 (2017).
73. Chen, R. et al. Graphitic carbon nitride nanosheet@metal-organic framework core-shell nanoparticles for photo-chemo combination therapy. *Nanoscale* **7**, 17299–17305 (2015).
74. Zhang, X. et al. Carbon nitride hollow theranostic nanoregulators executing laser-activatable water splitting for enhanced ultrasound/fluorescence imaging and cooperative phototherapy. *ACS Nano* **14**, 4045–4060 (2020).
75. Guo, L. et al. Incorporating TiO_2 nanotubes with a peptide of D-amino K122-4 (D) for enhanced mechanical and photocatalytic properties. *Sci. Rep.* **6**, 22247 (2016).
76. Cipriano, A., Miller, C. & Liu, H. Anodic growth and biomedical applications of TiO_2 nanotubes. *J. Biomed. Nanotechnol.* **10**, 2977–3003 (2014).
77. Yang, D. et al. Carbon-dot-decorated TiO_2 nanotubes toward photodynamic therapy based on water-splitting mechanism. *Adv. Healthc. Mater.* **7**, 1800042 (2018).
78. Kim, W. et al. Role of HIF-1α in response of tumors to a combination of hyperthermia and radiation in vivo. *Int. J. Hyperth.* **34**, 276–283 (2018).
79. Maas, A. et al. Tumor vascular microenvironment determines responsiveness to photodynamic therapy. *Cancer Res.* **72**, 2079–2088 (2015).
80. Weiss, A. et al. Low-dose angiostatic tyrosine kinase inhibitors improve photodynamic therapy for cancer: lack of vascular normalization. *J. Cell. Mol. Med.* **18**, 480–491 (2014).
81. Tong, X. et al. Monitoring tumor hypoxia using (18)F-FMISO PET and pharmacokinetics modeling after photodynamic therapy. *Sci. Rep.* **6**, 36551 (2016).
82. Lee, S., Kim, J., Han, Y. & Cho, D. The effect of modulated electro-hyperthermia on temperature and blood flow in human cervical carcinoma. *Int J. Hyperthermia* **34**, 953–960 (2018).
83. Song, C., Park, H. & Griffin, R. Improvement of tumor oxygenation by mild hyperthermia. *Radiat. Res.* **155**, 515–528 (2001).
84. Shen, Z. et al. Tumor microenvironment-triggered nanosystems as dual-relief tumor hypoxia immunomodulators for enhanced phototherapy. *Theranostics* **10**, 9132–9152 (2020).
85. Cham, K. et al. Metronomic gemcitabine suppresses tumour growth, improves perfusion, and reduces hypoxia in human pancreatic ductal adenocarcinoma. *Br. J. Cancer* **103**, 52–60 (2020).
86. Chen, Q. et al. Drug-induced co-assembly of albumin/catalase as smart nanotheranostics for deep intra-tumoral penetration, hypoxia relieve, and synergistic combination therapy. *J. Control. Release* **263**, 79–89 (2020).
87. Mpekris, F., Baish, J., Stylianopoulos, T. & Jain, R. Role of vascular normalization in benefit from metronomic chemotherapy. *Proc. Natl Acad. Sci. USA* **114**, 1994–1999 (2017).
88. Shen, Y. et al. Tumor vasculature remolding by thalidomide increases delivery and efficacy ofcisplatin. *J. Exp. Clin. Cancer Res.* **38**, 427 (2019).
89. Yang, Z. et al. Defeating relapsed and refractory malignancies through a nano-enabled mitochondria-mediated respiratory inhibition and damage pathway. *Biomaterials* **229**, 119580 (2020).
90. Fan, X. et al. A mitochondria-targeted organic arsenical accelerates mitochondrial metabolic disorder and function injury. *Bioorg. Med. Chem.* **27**, 760–768 (2019).
91. Yang, Z. et al. Self-generating oxygen enhanced mitochondrion-targeted photodynamic therapy for tumor treatment with hypoxia scavenging. *Theranostics* **9**, 6809–6823 (2019).
92. Broekgaarden, M. et al. Inhibition of hypoxia-inducible factor 1 with acriflavine sensitizeshypoxic tumor cells to photodynamic therapy with zinc phthalocyanine-encapsulatingcationic liposomes. *Nano Res.* **9**, 1639–1662 (2019).
93. Esfahlan, R., Guardia, M., Ahmadi, D. & Yousefi, B. Modulating tumor hypoxia by nanomedicine for effective cancer therapy. *J. Cell Physiol.* **233**, 2019–2031 (2019).
94. Liu, P. et al. Oxygen-self-supplying and HIF-1α-inhibiting core−shell nanosystem for hypoxia-resistant photodynamic therapy. *ACS Appl. Mater. Interfaces* **11**, 48261–48270 (2019).
95. Ma, Q. et al. Cell-inspired all-aqueous microfluidics: from intracellular liquid-liquid phase separation toward advanced biomaterials. *Adv. Sci.* **7**, 1903359 (2020).
96. Huang, X. et al. Combined cancer chemo-photodynamic and photothermal therapy based on ICG/PDA/TPZ-loaded nanoparticles. *Mol. Pharm.* **16**, 2172–2183 (2019).

97. Ma, Q. et al. Microfluidic-mediated nano-drug delivery systems: from fundamentals to fabrication for advanced. *Nanoscale* **12**, 15499–15908 (2020).
98. Zhu, R. et al. Cancer-selective bioreductive chemotherapy mediated by dual hypoxia-responsive nanomedicine upon photodynamic therapy-induced hypoxia aggravation. *Biomacromolecules* **20**, 2649–2656 (2019).
99. Liu, Y. et al. Hypoxia induced by upconversion-based photodynamic therapy: towards highly effective synergistic bioreductive therapy in tumors. *Angew. Chem.* **127**, 8223–8227 (2015).
100. Cao, J. et al. Iodinated cyanine dyes for fast near-infrared-guided deep tissue synergistic phototherapy. *ACS Appl. Mater. Interfaces* **11**, 25720–25729 (2019).